

Uranyl bis-iminophosphorane complexes with in- and out-of-plane equatorial coordination †

Mark J. Sarsfield,^{a*} Helen Steele,^a Madeleine Helliwell^b and Simon J. Teat^c

^a Centre for Radiochemistry Research, Department of Chemistry, The University of Manchester, Manchester, UK M13 9PL.

E-mail: mark.j.sarsfield@man.ac.uk

^b Department of Chemistry, The University of Manchester, Manchester, UK M13 9PL

^c CLRC Daresbury Laboratory, Daresbury, Warrington, Cheshire, UK WA4 4AD

Received 25th April 2003, Accepted 16th July 2003

First published as an Advance Article on the web 29th July 2003

The new bis-iminophosphorane complexes $[\text{UO}_2\text{Cl}\{\eta^3\text{-CH}(\text{Ph}_2\text{PNSiMe}_3)_2\}(\text{thf})]$ (**1**) and $[\text{UO}_2\text{Cl}\{\eta^3\text{-N}(\text{Ph}_2\text{-PNSiMe}_3)_2\}(\text{thf})]$ (**2**) are synthesised from the reaction of $[\text{UO}_2\text{Cl}_2(\text{thf})_3]$ with $\text{Na}[\text{CH}(\text{Ph}_2\text{PNSiMe}_3)_2]$ (**NaI**) and $\text{Na}[\text{N}(\text{Ph}_2\text{PNSiMe}_3)_2]$ (**NaII**), respectively. Both **1** and **2** form dinuclear complexes in the absence of a coordinating solvent. The reactivity of **1** has been explored. The crystal structures of **1** and **2** have been determined. They display distorted pentagonal bipyramidal geometry with ligands **I** and **II** both bonding in a tridentate chelating manner which is shown to remain intact in solution. Complex **1** contains a U–C bond that is out of the equatorial plane by 0.842(3) Å in contrast to **2** where the U–N bond is close to the equatorial plane (0.154(3) Å). This difference in geometry results in an unusual low energy electronic absorption band for **1** originating from C → U LMCT supported by molecular orbital calculations at the DFT level.

Introduction

Uranium U(VI) chemistry is dominated by the uranyl ion, $[\text{UO}_2]^{2+}$, the stability of which comes from the overlap of six combinations of oxygen 2p orbitals and six uranium based 5f/6d orbitals to give a linear O=U=O unit.^{1,2} Uranyl complexes generally adopt a bipyramidal geometry with 3–6 additional ligands bonded in the equatorial plane. Whilst a convincing conceptual model of the axial O=U=O bonding has been established,^{1,3,4} the role of the remaining orbitals (mainly 5f/6d based) in equatorial bonding is unclear. Recent investigations show that some electron rich equatorial ligands can influence axial U=O bonding although there is conflicting evidence as to the mechanism involved. For example, under strong alkaline conditions $[\text{UO}_2(\text{OH})_4]^{2-}$ is formed with a weakening and lengthening of the oxo bonds ascribed to competition for 6d orbital overlap between axial oxo and equatorial hydroxyl oxygen orbitals.⁵ Alternatively, IR⁶ and Raman⁷ spectroscopy of uranyl compounds supports a relationship between the basicity of equatorial ligands and the strength of the uranium–oxo bonds through destabilisation of the HOMO (σ_u) orbital.¹ Both mechanisms may explain the decrease in O=U=O stretching vibration frequencies of the monomeric amido $[\text{UO}_2\text{L}_2\text{-}(\text{NSiMe}_3)_2]$ (L = thf, Ph_3PO)^{8,9} and alkoxo $[\text{UO}_2\text{L}_n(\text{OR})_2]$ (L = thf, Ph_3PO , py; R = C(CF₃)₃, ^tBu, CH(^tBu)Ph, CH(Ph)₂, 2,6-^tBu₂C₆H₃, 2,6-ⁱPr)^{8–12} complexes.

To probe these destabilisation effects further, we are exploring how ligands with different coordination modes and electron donating ability influence the bonding in uranyl systems. Recently, we reported a complex containing the bis-iminophosphorano ligand $[\text{CH}(\text{Ph}_2\text{PNSiMe}_3)_2]^-$ [**I**].¹³ All reported metal complexes containing **I** exhibit coordination through two nitrogens to form a chelate ring in a twist-boat conformation that may or may not involve bonding to the central carbon atom.^{13–19} When M–C coordination occurs the three coordinating ligand atoms and the metal centre cannot all lie in

the same plane (Fig. 1). In the case of uranyl, the metal centre can stabilise the ligand charge by forming a U–C bond only at the expense of unfavourable out-of-plane equatorial coordination. Both U–C bonding and out-of-plane equatorial coordination are rare for uranyl (U(VI)) complexes. Here we explore the reactivity and spectroscopic properties such as an unusual bonding mode imposes and include molecular modelling investigations, at the DFT level, to help understand the observed influences on electronic structure.

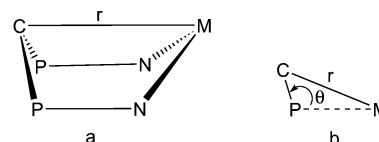


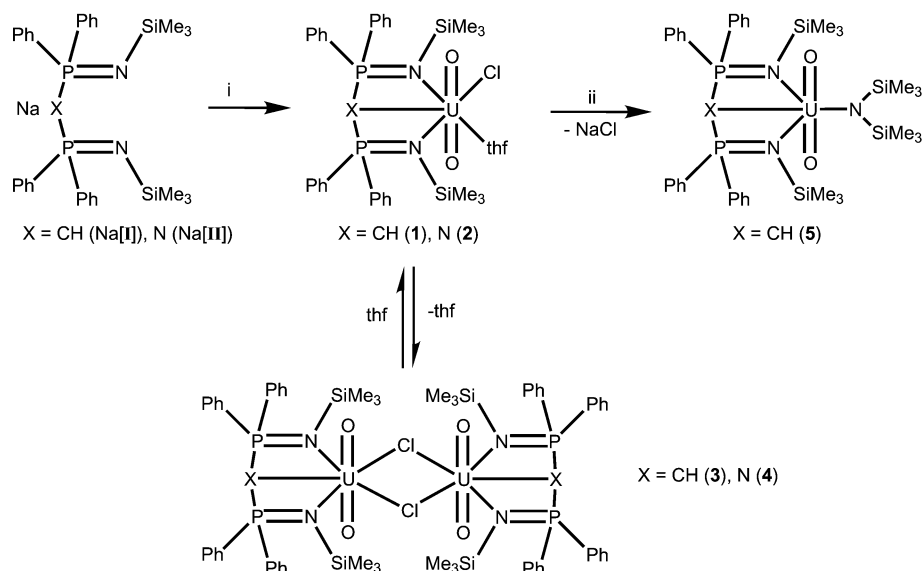
Fig. 1 (a) Boat conformation of the six membered chelate ring in complexes of **I**; (b) torsional angle viewed down the axis defined by the two P atoms.

Results and discussion

Synthesis

The complex $[\text{UO}_2\text{Cl}_2(\text{thf})_3]$,²⁰ soluble in thf, provides a convenient route into non-aqueous uranyl chemistry and was used to prepare $[\text{UO}_2\text{Cl}\{\eta^3\text{-CH}(\text{Ph}_2\text{PNSiMe}_3)_2\}(\text{thf})]$ (**1**), by metathesis reactions with the sodium salt of $[\text{CH}(\text{Ph}_2\text{PN-SiMe}_3)_2]^-$ [**I**] (Scheme 1). In the absence of a coordinating solvent, such as thf, the dimeric compound $[\text{UO}_2\text{Cl}\{\eta^3\text{-CH}(\text{Ph}_2\text{-PNSiMe}_3)_2\}]_2$ (**3**) was crystallised from dichloromethane solutions and is reported elsewhere as a uranyl complex containing a C–U(VI) bond.¹³ The carbon–U(VI) bond length in **3** is quite long (2.695(12) Å) and it could be argued that the compound is zwitterionic with substantial negative charge residing on the carbon. Surprisingly, thf or dichloromethane solutions of **1** or **3**, respectively, are unreactive towards electrophiles such as MeI, a reaction that occurs readily with the ligand **NaI**, and do not undergo insertion reactions with isocyanates.¹⁸ However, substitution of the terminal chloride in **1** by the bulky bis-trimethylsilylamide ligand gave the six coordinate species $[\text{UO}_2\{\text{N}(\text{SiMe}_3)_2\}\{\eta^3\text{-CH}(\text{Ph}_2\text{PNSiMe}_3)_2\}]$ (**5**).

† Electronic supplementary information (ESI) available: Variable temperature ¹H NMR spectra; Raman spectra; solid state diffuse reflectance electronic absorption spectra; luminescence spectra; interatomic distances of the optimised structures of **1*** and **2*** from molecular modelling calculations. See <http://www.rsc.org/suppdata/dt/b3/b304602h/>



Scheme 1 Formation of complexes 1–5; (i) $[\text{UO}_2\text{Cl}_2(\text{thf})_3]$, (ii) $\text{Na}\{\text{N}(\text{SiMe}_3)_2\}$.

All complexes were fully characterised by elemental analysis (C, H, N, Cl, P, U), ^1H , $^{13}\text{C}\{^1\text{H}\}$ and $^{31}\text{P}\{^1\text{H}\}$ NMR and Raman spectroscopy (see Experimental section). The CH coupling constant of the central carbon atom is sensitive to hybridisation of the carbon based orbitals and in **5** ($^1J_{\text{CH}} = 132$ Hz) is similar to that of **1** ($^1J_{\text{CH}} = 136$ Hz) but intermediate between the that of the neutral ligand $\text{CH}_2(\text{Ph}_2\text{PNSiMe}_3)_2$ ($^1J_{\text{CH}} = 124$ Hz) and Na[I] ($^1J_{\text{CH}} = 144$ Hz). The amido complex **5** exhibits some fluxionality in CD_2Cl_2 solution on the NMR time scale. There are two different pairs of SiMe_3 groups in **5**; two on the tridentate ligand and two on the amido group ($\text{N}(\text{SiMe}_3)_2$). This is reflected in the ^1H NMR spectrum at room temperature which contains a broad singlet (δ 0.42, $\text{N}(\text{SiMe}_3)_2$) and a sharp singlet (δ 0.07, $\text{P}=\text{NSiMe}_3$) together with one broad peak for the aryl protons (δ 7.40). Two different SiMe_3 groups are also observed in the ^{13}C (δ 0.58, 5.6) and ^{29}Si (δ -4.9, -3.4) NMR spectra. On cooling the solution to -40 °C ^1H NMR spectroscopy shows that the broad singlet at δ 0.42 becomes two peaks each representing 9H relative to the $\text{P}=\text{NSiMe}_3$ (18H) signal, which remains a single sharp peak. Likewise, the aryl protons resolve to two sets of phenyl ring protons (see ESI†). This behavior is consistent with restricted rotation of the amido group about the U–N bond placing one of the SiMe_3 groups in close proximity to one set of Ph groups (Si(2) and *ipso*-C(14), C(8), see Fig. 3 and discussion below).

To assess the generality for out-of-plane bonding using ligand frameworks of type **I** we have also employed $[\text{N}(\text{Ph}_2\text{PNSiMe}_3)_2]^-$ (**II**), readily synthesised using a modified literature procedure,^{21,22} replacing the central carbon in **I** with nitrogen. Combining thf solutions of **II** and $[\text{UO}_2\text{Cl}_2(\text{thf})_3]$ results in an immediate colour change from pale to dark yellow and a downfield shift in the ^{31}P NMR spectra from $\delta_{\text{p}} 6.3$ (**II**) to 10.2 $[\text{UO}_2\text{Cl}\{\eta^3\text{-CH}(\text{Ph}_2\text{PNSiMe}_3)_2\}(\text{thf})]$ (**2**). Recrystallisation of **2** from thf provides crystals of sufficient quality for a complete X-ray diffraction study. Recrystallisation of **2** from dichloromethane gave crystals that analyse correctly for the chloro-bridged dimer $[\text{UO}_2\text{Cl}\{\eta^3\text{-CH}(\text{Ph}_2\text{PNSiMe}_3)_2\}]_2 \cdot \frac{1}{2}\text{CH}_2\text{Cl}_2$ ($4 \cdot \frac{1}{2}\text{CH}_2\text{Cl}_2$) a compound that is only sparingly soluble in dichloromethane. Adding thf to a suspension of **4** in CD_2Cl_2 the mononuclear uranyl complex **2** was regenerated; identified in solution by coordinated thf signals in the ^1H and ^{13}C NMR spectra ($\delta_{\text{H}} = 1.55, 3.60$; $\delta_{\text{C}} = 25.8, 67.6$) demonstrating the reversibility of monomer/dimer formation.

Molecular structures of 1 and 5

The synthesis and structure of **3** are discussed elsewhere.¹³ Addition of an excess of thf to a solution of **3** in dichloro-

methane converts the chloro-bridged dimer to **1**. This is confirmed in the crystal structure of **1** presented in Fig. 2 with crystallographic data and selected bond lengths and angles listed in Tables 1 and 2, respectively. Suitable crystals of **1** were grown from thf at -15 °C and crystallised in the monoclinic space group $P2_1/c$, with two molecules of **1** and two molecules of non-bonded thf in the asymmetric unit. The uranium atom lies at the centre of a pentagonal bipyramidal structure with the axial oxo ligands significantly bent from linearity (O(1)–U–O(2) $175.12(13)^\circ$) and the U=O bonds (U–O(1) 1.773(3) Å, U–O(2) 1.783(3) Å) are similar to those in **3** (U–O 1.763(6), 1.764(6) Å). A coordinated chloride and a thf oxygen occupy the inner coordination sphere together with a tridentate bis-iminophosphorano ligand bonded to uranium through two nitrogen and one out-of-plane carbon atom. The U–O(thf) (2.467(3) Å) and U–Cl (2.6806(11) Å) bond distances are similar to those reported for $[\text{UO}_2\text{Cl}_2(\text{thf})_2]_2$ (U–Cl(terminal) 2.66(3) Å, U–O(thf) (2.32(3)–2.49(4) Å)) and $[\text{UO}_2\text{Cl}_2(\text{thf})_3]$ (U–Cl 2.698(2), 2.687(2) Å, U–O(thf) (2.467(6)–2.443(6) Å)). The displacement of the central carbon C(1) from a least squares plane defined by U(1), N(1), N(2), Cl(1) and O(3)

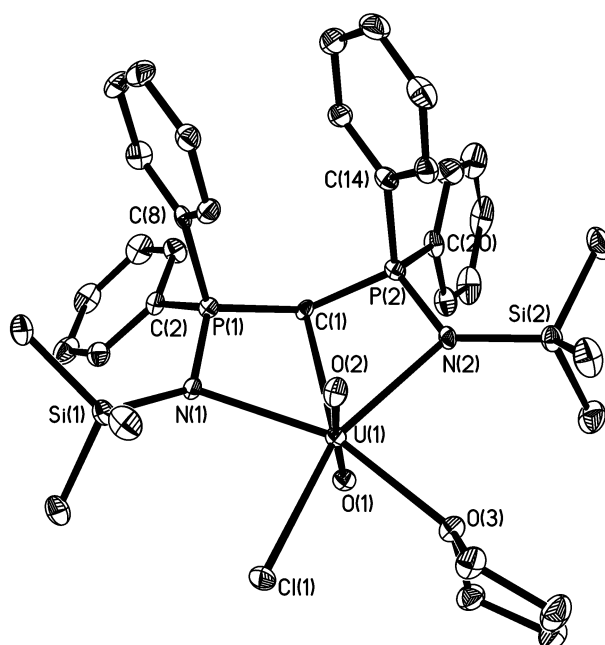


Fig. 2 ORTEP diagram of complex **1** with 50% probability ellipsoids (hydrogen atoms omitted for clarity).

Table 1 Crystallographic data for complexes **1**, **2**, **4** and **5**

	1 ·thf	2	4 ·½CH ₂ Cl ₂	5 ·½toluene
Formula	C ₃₉ H ₅₅ ClN ₂ O ₄ P ₂ Si ₂ U	C ₃₄ H ₄₆ ClN ₃ O ₃ P ₂ Si ₂ U	C _{60.5} H ₇₇ Cl ₃ N ₆ O ₄ P ₄ Si ₄ U ₂	C _{40.5} H ₆₁ N ₃ O ₂ P ₂ Si ₄ U
<i>M</i>	1007.45	936.34	1770.93	1034.25
Crystal system	Monoclinic	Triclinic	Triclinic	Triclinic
<i>a</i> /Å	20.410(3)	10.999(1)	11.295(2)	10.2914(13)
<i>b</i> /Å	24.902(4)	12.595(1)	12.479(2)	12.7639(16)
<i>c</i> /Å	16.987(3)	16.098(2)	14.211(3)	17.868(2)
<i>a</i> ^o	–	73.384(2)	107.595(3)	84.831(2)
<i>β</i> ^o	101.577(3)	74.307(2)	93.089(3)	83.767(2)
<i>γ</i> ^o	–	64.549(1)	103.350(3)	77.728(2)
<i>V</i> /Å ³	8458(2)	1901.3(3)	1841.2(6)	2274.5(5)
<i>T</i> /K	100(2)	100(2)	150(2)	100(2)
Space group	<i>P</i> 2 ₁ / <i>c</i>	<i>P</i> $\bar{1}$	<i>P</i> $\bar{1}$	<i>P</i> $\bar{1}$
<i>Z</i>	8	2	1	2
μ (Mo-K α)/mm ⁻¹	4.074	4.523	4.698	3.780
Collected reflections	38900	15229	8211	19949
Unique reflections (<i>R</i> _{int})	16867 (0.0354)	7674 (0.0376)	5977 (0.0500)	10410 (0.0297)
<i>R</i> 1 [<i>I</i> > 2 σ (<i>I</i>)]	0.0367	0.0249	0.0718	0.0291
<i>wR</i> 2 [<i>I</i> > 2 σ (<i>I</i>)]	0.0924	0.0565	0.1848	0.0640

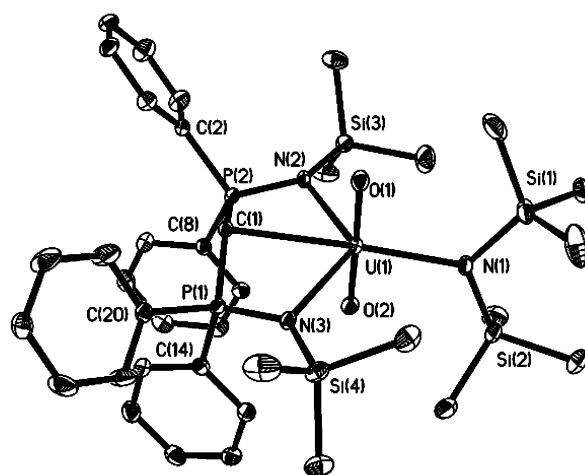
Table 2 Selected interatomic distances (Å) and bond angles (°) for **1**, **2**, **4** and **5**

	1	2	4	5	
U–O(1)	1.773(3)	U–O(1)	1.778(2)	U–O(1)	1.774(2)
U–O(2)	1.783(3)	U–O(2)	1.771(2)	U–O(2)	1.784(2)
U–O(3)	2.467(3)				
U–Cl(1)	2.681(1)	U–Cl(1)	2.6724(8)	U–Cl(1)	2.795(3)
				U–Cl(1A)	2.812(3)
U–N(1)	2.510(3)	U–N(1)	2.556(3)	U–N(1)	2.593(11)
U–N(2)	2.528(3)	U–N(3)	2.547(3)	U–N(3)	2.528(10)
U–C(1)	2.707(4)	U–N(2)	2.459(3)	U–N(2)	2.442(11)
N(1)–P(1)	1.597(4)	N(1)–P(1)	1.584(3)	N(1)–P(1)	1.600(12)
N(2)–P(2)	1.601(4)	N(3)–P(2)	1.598(3)	N(3)–P(2)	1.568(10)
O(1)–U–O(2)	175.1(1)	O(1)–U–O(2)	174.9(1)	O(1)–U–O(2)	178.3(4)
P(1)–C(1)–P(2)	139.0(3)	P(1)–N(2)–P(2)	158.0(2)	P(1)–N(2)–P(2)	157.4(8)
P(1)–N(1)–U	100.2(2)	P(1)–N(1)–U	97.3(1)	P(1)–N(1)–U	94.7(5)
P(2)–N(2)–U	99.3(2)	P(2)–N(3)–U	97.0(1)	P(2)–N(3)–U	98.6(5)
				P(2)–N(2)–U	100.8(1)
				P(1)–N(3)–U	98.9(1)

(0.842(3) Å) is similar to that in **3** (0.8877(96) Å).¹³ The only other reported uranyl complex with an atom bonded to uranium that is significantly displaced from the equatorial plane, [UO₂·{(OCH₂)₂CH–HOC₆H₂Cl(CH=N(CH₂)₂)₂S}],²³ contains a sulfur atom 1.25 Å above the equatorial plane, but there is some doubt as to whether this is a bonding interaction (U–S, 3.003(3) Å).

Substitution of the terminal chloride with the bulky amido group [N(SiMe₃)₂][–] gives **5** (Scheme 1) crystallised from toluene in the triclinic space group *P* $\bar{1}$, with one molecule of **5** in the asymmetric unit (Fig. 3). The interatomic bond distances and angles for **1** and **5** are similar (Table 2) except for a more linear O=U=O bond angle (O(1)–U–O(2) 178.16(10)^o *cf.* 175.12(13)^o for **1**). However, the U–N(SiMe₃)₂ bond (U–N(1) 2.291(3) Å) is much shorter than the U–N bonds between uranium and the bis-iminophosphorano ligand (U–N(2) 2.495(3) Å, U–N(3) 2.484(3) Å) and is comparable to the only other uranyl–amido crystal structure to be determined, Na(thf)₂[UO₂(NSiMe₃)₃] (2.305(4)–2.318(4) Å).²⁴ In **5**, there is restricted rotation about the U–N(SiMe₃)₂ bond, reflected in the variable temperature NMR data (discussed earlier). Freezing the rotation of the amido group places one of the SiMe₃ groups in close proximity to two Ph groups and is corroborated by comparing the distance between the Ph ring carbons and the two spatially different SiMe₃ groups (Si(1)–C(20) 7.719(5), Si(1)–C(2) 7.719(5), Si(2)–C(14) 6.164(5), Si(2)–C(8) 6.819(5) Å).

Bonding between uranium and carbon is well known in U(IV) complexes,^{25–27} but U(VI)–C bonds are rare so confirmation of the presence of such a bond is desirable. Metal complexes containing the bis-iminophosphorano ligand **1** all contain a six-membered chelate ring in a boat conformation^{14,15,17–19}

**Fig. 3** ORTEP diagram of complex **5** with 50% probability ellipsoids (hydrogen atoms omitted for clarity).

(Fig. 1(a)) with the P–C–P fragment bent towards the metal centre depending on the degree of M–C interaction, thus, the torsion angle (θ , Fig. 1(b)) M–P(1)–P(2)–C(1) provides an indicator of the M–C bonding. For M = Al there is no M–C bonding (θ = 113.47(17), Al–C = 3.002(3) Å) whereas complexes **1**, **3** and **5** all show a preference for the central carbon atom to be bent towards the uranium centre (θ = 78.34(39), 80.98(121) and 80.33(28)^o, respectively) despite the electrostatic repulsions from the axial oxygen atoms.

Molecular structure of 2 and 4

X-Ray quality crystals of $[\text{UO}_2\text{Cl}\{\eta^3\text{-N}(\text{Ph}_2\text{PNSiMe}_3)_2\}(\text{thf})]$ (**2**) were obtained from a saturated thf solution standing at -15°C for three days. An ORTEP representation of the molecular structure of **2** giving the atom-numbering scheme used in Table 2, is depicted in Fig. 4. The structure consists of a seven-coordinate uranium centre with the oxo ligands occupying the axial positions of a distorted pentagonal bipyramidal geometry. The five equatorial positions are occupied by three nitrogen atoms from **II**, the thf oxygen atom and a terminal chloride.

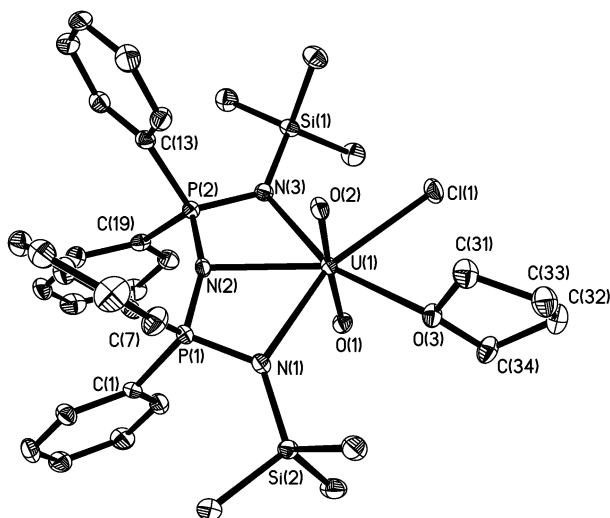


Fig. 4 ORTEP diagram of complex **2** with 50% probability ellipsoids (hydrogen atoms omitted for clarity).

X-Ray quality crystals of $[\text{UO}_2\text{Cl}\{\eta^3\text{-N}(\text{Ph}_2\text{PNSiMe}_3)_2\}]_2$ (**4**) were obtained from a saturated dichloromethane solution at -15°C . An ORTEP diagram of the structure of **4** is depicted in Fig. 5. The structure consists of two distorted pentagonal bi-pyramidal uranyl units each bridged by two chlorine atoms in a centrosymmetric dimer. Each uranyl group is bonded to a tridentate bis(iminophosphorano)amide ligand through two nitrogen donor atoms and a central nitrogen atom. The most striking features about the structures of **2** and **4** are the bonding of the tridentate bis-iminophosphorano ligand compared to complexes **1**, **3** and **5**. In compounds **2** and **4**, the coordinating atoms N(1), N(2) and N(3) in the bis(iminophosphorano)amide ligand are all relatively close to the uranyl equatorial plane. The

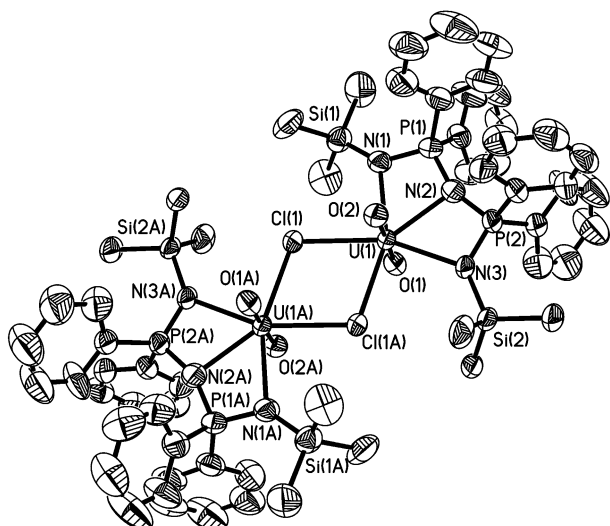


Fig. 5 ORTEP diagram of complex **4** with 50% probability ellipsoids (hydrogen atoms omitted for clarity).

Table 3 Stretching vibrations of the uranyl unit for **1–5**

Complex	IR (Nujol)	Raman (solid)	Raman (solution)
	O=U=O (ν_3)	O=U=O (ν_1)	
1	908	825	827 ^a
2	909	829	835 ^a
3	924	836	— ^b
4	924	846	— ^b
5	918	823	818 ^c

^a In thf. ^b Not soluble enough for solution study. ^c In dichloromethane.

displacement of N(2) from the plane defined by (N(1), N(3), Cl(1), U(1)) (**2** 0.154(3), **4** 0.146(12) Å) are considerably less than the displacement of the central carbon atom from a similarly defined plane in complexes **1**, **3** and **5**. Also, the central nitrogen is pulled inwards towards uranium, so much so that the central nitrogen is closer to the metal centre (U–N(2), **2**: 2.459(3), **4**: 2.442(11)) than the P=N nitrogen atoms (U–N(1), **2**: 2.556(4), **4**: 2.593(11); U–N(3), **2**: 2.547(3), **4**: 2.528(10)). This difference in bonding is also apparent in the U–N–P and P–X–P (X = CH, N) bond angles (Table 2). The only other structurally characterised metal complexes containing the bis(iminophosphorano)amide ligand **II** are $[\text{MMe}_2\{\text{N}(\text{Ph}_2\text{PNSiMe}_3)_2\}]$ (M = Al, In); they possess similar P=N bond lengths, but do not display a M–N_{central} bond, evident in the M–N_{central} bond lengths and N=P–N_{central}–P torsion angles (M = Al: 3.022(10) Å, 31.86(27)°; In: 3.505(3) Å, 25.52(34)°);²¹ (**2**: 2.459(3) Å, 198.51(53)°; **4**: 2.442(11) Å, 185.49(225)°).

Vibration and electronic spectroscopy

Raman spectroscopy provides a more sensitive probe of the O=U=O bond strength than crystallographic studies and changes in the uranyl coordination sphere can be detected easily.^{6,28–30} For example, the uranyl–oxo symmetric stretch in the Raman spectra of **1** and **2** (825 and 829 cm^{-1} , respectively) are significantly shifted to higher energy for the related chloro-bridged dimers **3** and **4** (836 and 846 cm^{-1} , respectively). A comparison of the solid and solution state Raman spectra of **1**, **2** and **5** shows little change in the oxo symmetric stretching frequencies suggesting that the coordination sphere around the uranium centre for these compounds remains intact in solution (Table 3) (for spectra see ESI †).

Considering the dramatic change in molecular structure around the metal coordination sphere on changing the central coordinating atom of the bis-iminophosphorano ligand from CH (**1** and **3**) to N (**2** and **4**) it is not surprising to find vastly different spectroscopic properties. Indeed, the red colour of **1** and **3** compared to the yellow of **2** and **4** are obvious indications of this. The room-temperature electronic absorption spectra of **1** and **2** in thf (400–600 nm) are compared in Fig. 6. The absorption spectrum of **2** in thf shows a peak with maximum intensity at 444 nm ($\epsilon = 112 \text{ dm}^3 \text{ mol}^{-1} \text{ cm}^{-1}$) with well resolved vibrational fine structure. The solid-state diffuse reflectance absorption spectrum is essentially the same except for a 5 nm red shift for each of the vibronic bands (see ESI †). The fine structure observed for **2** is typical for a uranyl complex and originates from progressions in the symmetric O=U=O stretch for the excited state.³¹ In contrast to **2**, **1** possesses two broad absorptions at 424 nm ($\epsilon = 650 \text{ dm}^3 \text{ mol}^{-1} \text{ cm}^{-1}$) and 492 nm ($\epsilon = 388 \text{ dm}^3 \text{ mol}^{-1} \text{ cm}^{-1}$) with poorly resolved fine structure only observed on the former. Cooling a sample of **1** in thf to -100°C does not measurably increase the resolution of these bands. The solid-state diffuse reflectance absorption spectrum clearly shows the 493 nm band but the signal at 424 nm could not be observed due to the limitations of the instrument used (see ESI †).

This fundamental difference in electronic structure between **1** and **2** is also evident in emission spectroscopy (see ESI †); for **2**

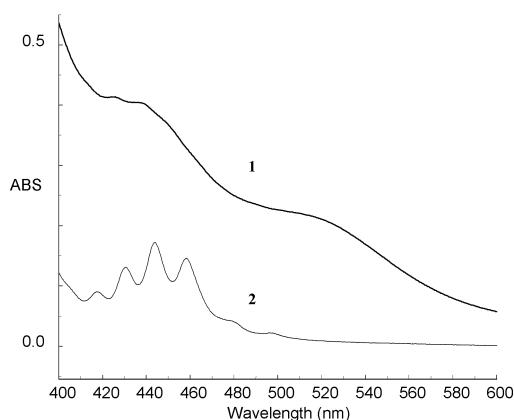


Fig. 6 Room-temperature absorption spectra of **1** (1.49 mM, in thf) and **2** (1.78 mM, in thf).

a broad but structured band is present whereas for **1** there is no detectable luminescence and only Raman bands from the solvent are observed.

Molecular modelling and orbital calculations

An insight into the bonding and electronic structure of the tridentate bis-iminophosphorano complexes may be obtained from molecular modelling. Electronic calculations were performed using a DFT approach employing a relativistic basis set for the uranium centre and a 6-31G* basis set on all remaining atoms. The coordinates of the crystal structures were used as a starting point for the optimisations. To reduce the computational expense each phenyl group in **1** and **2** was replaced by a methyl prior to optimisation (defined as **1*** and **2***, respectively). Very good structural agreement was found for both complexes (see ESI†). The U–C_{central} and U–N_{central} separations were calculated to be 2.753 and 2.567 Å, respectively (cf. 2.707(4) (**1**); 2.459(3) (**2**)).

The HOMO of **1*** consists of mainly a non-bonding orbital with a large proportion of the electron density residing on C_{central} in a p-type orbital pointing towards the uranium centre (Fig. 7). Excitation of an electron from this orbital to the LUMO, normally a uranium based 5f orbital,¹ may result in a transfer of charge to the uranium centre. Thus, the lowest energy electronic absorption band for **1** (Fig. 6, 493 nm) can be explained in terms of a C → U LMCT within the uranyl system.

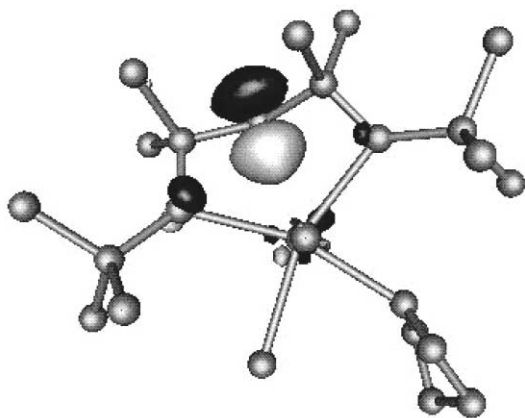


Fig. 7 Molecular orbital representation of the HOMO of **1***.

It is apparent from these results that non-aqueous chemistry of the uranyl ion can provide some unique coordination geometries and in utilising ‘non-traditional’ ligands, the electronic properties of uranyl compounds can be perturbed.

Changes to the coordination sphere (CH for N) result in different geometric and electronic properties of uranyl complexes that are related to out-of-plane equatorial bonding.

Experimental section

General

Sodium bis-trimethylsilylamide (BDH) was used as received. The ligand precursors CH₂(Ph₂PNSiMe₃)₂³³ and NH(Ph₂PNSiMe₃)₂²¹ were synthesised according to the literature. Sodium salts of **1** and **2** were prepared by a slightly modified literature procedure using sodium bis-trimethylsilylamide as a base instead of NaH.¹⁶ The synthesis of **3** is described elsewhere.¹³ All reactions and manipulations were performed under argon using standard Schlenk techniques or an inert atmosphere dry-box. Solvents were purified by distillation from sodium (toluene), sodium/benzophenone ketyl (thf) and P₂O₅ (CH₂Cl₂) and stored over molecular sieves (4 Å). ¹H, ¹³C{¹H} and ³¹P{¹H} NMR spectra were recorded on a Bruker Avance 400 instrument at 400 MHz, 100 MHz and 162 MHz, respectively. Raman and UV/VIS spectroscopy were recorded on a Bruker Equinox 55 FTIR/Raman and Varian Cary 500 instruments, respectively. Luminescence measurements were made on a Perkin-Elmer LS 55. Elemental analysis was performed on a Carlo ERBA Instruments CHNS-O EA1108 Elemental Analyser for C, H and N and by a Fisons Horizon Elemental Analysis ICP-OED spectrometer for U and P.

Preparation of [UO₂Cl{η³-CH(Ph₂PNSiMe₃)₂}(thf)] **1**

A solution of [UO₂Cl₂(thf)₂]₂ (1.21 g, 2.50 mmol) in thf (50 cm³) was treated with a toluene (50 cm³) solution of Na[CH(Ph₂PNSiMe₃)₂] (5.00 mmol) and stirred at ambient temperature for 30 min. The resulting deep red solution was evaporated *in vacuo* and the red oily residue extracted with dichloromethane (3 × 30 cm³). The solvent was removed *in vacuo*, and the residue dissolved in a minimum amount of thf followed by cooling to –15 °C for 7 days to give red crystals of **1**. Yield 0.980 g, 70%. (Found: C, 46.04; H, 5.01; N, 2.77; Cl, 3.72; P, 6.42; U, 24.07. C₃₉H₅₅ClN₂O₄P₂Si₂U (1·thf) requires C, 46.50; H, 5.50; N, 2.78; Cl, 3.52; P, 6.15; U, 23.63%). Raman (solid in glass capillary) (1600–600 cm⁻¹): 1590 (s), 1572, 1188 (w), 1116 (w), 1028 (m), 1000 (vs), 912 (w), 825 (s), 777 (w), 663 (w), 618 (m). δ_H (400 MHz, thf-d₈, 25 °C, TMS): 0.20 (s, 18H, SiMe₃), 1.75 (m, CH₂-thf), 2.28 (t, 1H, CH, J_{HP} = 11 Hz), 3.62 (m, CH₂-thf), 7.22 (m, 8H, *o*-Ph), 7.35 (m, 4H, *p*-Ph), 7.73 (m, 8H, *m*-Ph); δ_C (100 MHz, thf-d₈, 25 °C, TMS): 0.1 (SiMe₃), 19.5 (d,t, CH, J_{CH} = 138 Hz, J_{CP} = 116 Hz), 21.7 (CH₂-thf), 63.6 (CH₂-thf), 124.1 (t, *o*-Ph, J_{CP} = 12 Hz), 127.1 (s, *p*-Ph), 128.1 (m, *m*-Ph), 132.9 (d, *ipso*-Ph, J_{CP} = 101 Hz); δ_P (162 MHz, thf-d₈, 25 °C, 85% H₃PO₄), 8.0.

Preparation of [UO₂Cl{η³-N(Ph₂PNSiMe₃)}(thf)] **2**

A solution of [UO₂Cl₂(thf)₂]₂ (1.000 g, 1.03 mmol) in thf (50 cm³) was treated with a thf (50 cm³) solution of Na[N(Ph₂PNSiMe₃)₂] (1.862 g, 3.20 mmol) and stirred at ambient temperature for 4 h. The resulting yellow solution was evaporated *in vacuo* and the yellow solid extracted with dichloromethane (4 × 50 cm³). The solvent was removed *in vacuo* and the yellow solid recrystallised from thf yield (0.737 g, 71%) (Found: C, 44.81; H, 4.74; N, 4.33; Cl, 3.81; P, 7.03; U, 23.89. C₃₆H₅₀ClN₃O_{3.5}P₂Si₂U (2·½thf) requires C, 44.47; H, 5.18; N, 4.32; Cl, 3.65; P, 6.37; U, 24.48%). Raman (solid in glass capillary) (1600–600 cm⁻¹): 1591 (s), 1573 (w), 1187 (w), 1142 (w), 1105 (w), 1026 (m), 1000 (vs), 829 (s), 625 (m), 610 (m). δ_H (400 MHz, thf-d₈, 25 °C, TMS): 0.18 (s, 18H, SiMe₃), 1.55 (m, CH₂-thf), 3.60 (m, CH₂-thf), 7.16 (m, 8H, *o*-Ph), 7.39 (m, 4H, *p*-Ph), 7.56 (m, 8H, *m*-Ph); δ_C (100 MHz, thf-d₈, 25 °C, TMS), 3.9 (SiMe₃), 25.8 (CH₂-thf), 67.6 (CH₂O-thf), 128.0 (t, *o*-Ph,

$J_{CP} = 6$ Hz), 131.4 (s, *p*-Ph), 131.9 (t, *m*-Ph, $J_{CP} = 6$ Hz), 132.9 (dd, *ipso*-Ph, $J_{CP} = 112$, 2 Hz); δ_P (162 MHz, thf- d_8 , 25 °C, 85% H_3PO_4), 9.9.

Preparation of $[UO_2Cl\{\eta^3-N(Ph_2PNSiMe_3)_2\}]_2 \mathbf{4}$

A solution of $[UO_2Cl_2(thf)_2]_2$ (0.775 g, 0.80 mmol) in thf (50 cm^3) was treated with a thf (50 cm^3) solution of $Na[N(Ph_2PNSiMe_3)_2]$ (0.930 g, 1.60 mmol) and stirred at ambient temperature for 4 h. The resulting yellow solution was evaporated *in vacuo* and the yellow solid extracted with dichloromethane (4 \times 50 cm^3). The solvent was reduced in volume (~100 cm^3) *in vacuo*, followed by cooling to 5 °C for 7 days to give yellow crystals of **4**. Yield 0.955 g, 0.54 mmol, 67% (Found: C, 41.16; H, 4.34; N, 4.71; P, 7.19; U, 26.12. $C_{60.5}H_{77}Cl_3N_6O_4P_4Si_4U_2$ ($4 \cdot \frac{1}{2}CH_2Cl_2$) requires C, 41.03; H, 4.38; N, 4.75; P, 7.00; U, 26.88%). Raman (solid in glass capillary) (1600–600 cm^{-1}): 1590 (vs), 1574 (m), 1408 (w), 1186 (w), 1158 (w), 1136 (w), 1103 (w), 1028 (m), 1001 (vs), 846 (s), 780 (w), 685 (w), 654 (m), 611 (m).

Preparation of $[UO_2\{N(SiMe_3)_2\}\{\eta^3-CH(Ph_2PNSiMe_3)_2\}] \mathbf{5}$

A tetrahydrofuran solution of sodium bis-trimethylsilylamide (0.227 g, 2.06 mmol) was added to a tetrahydrofuran solution of **1** prepared *in situ* ($[UO_2Cl_2(thf)_2]_2$, 1.000 g, 1.03 mmol; $Na[CH(Ph_2PNSiMe_3)_2]$, 1.195 g, 2.06 mmol) at ambient temperature. The reaction mixture was stirred for 30 min followed by removal of solvent *in vacuo* and extraction of the residue into toluene. Filtration *via* cannula, concentration of the solution to half volume and cooling to –15 °C for 2 days gave orange crystals of **5** (yield, 0.330 g, 16%) (Found: C, 45.51; H, 5.67; N, 3.78; P, 5.95; U, 23.78. $C_{37}H_{57}N_3O_2P_2Si_4U$ requires C, 44.97; H, 5.81; N, 4.25; P, 6.27; U, 24.09%). Raman (solid in glass capillary) (1600–600 cm^{-1}): 1590 (s), 1576 (w), 1408 (w), 1182 (w), 1030 (m), 1000 (vs), 823 (s), 686 (w), 658 (w), 617 (w). δ_H (400 MHz, CD_2Cl_2 , –40 °C, TMS): 0.07 (s, 18H, $SiMe_3$), 0.37 (s, 9H, $SiMe_3$), 0.49 (s, 9H, $SiMe_3$), 2.61 (t, 1H, CH, $J_{HP} = 12$ Hz), 6.77 (m, 4H, *o*-Ph), 7.06 (br s, 4H, *m*-Ph), 7.11 (t, 2H, *p*-Ph, $J_{HP} = 7$ Hz), 7.57 (m, 6H, *p*-Ph and *o*-Ph), 7.80 (m, 4H, *m*-Ph). δ_C (100 MHz, CD_2Cl_2 , –40 °C, TMS): 3.0 ($SiMe_3$), 7.2 ($SiMe_3$), 7.5 ($SiMe_3$), 20.8 (dt, CH, $J_{CH} = 132$, $J_{CP} = 122$ Hz), 128.1 (t, *o*-Ph, $J_{CP} = 6$ Hz), 129.6 (t, *o*-Ph, $J_{CP} = 6$ Hz), 131.8 (s, *p*-Ph), 132.1 (t, *m*-Ph, $J_{CP} = 5$ Hz), 132.4 (s, *p*-Ph), 133.7 (br s, *m*-Ph), 138.8 (dd, *ipso*-Ph, $J_{CP} = 139$, 2 Hz). δ_P (162 MHz, CD_2Cl_2 , –40 °C, 85% H_3PO_4) 11.7 (s).

Crystal structure determination

The X-ray diffraction study for all compounds was carried out on a Bruker AXS SMART diffractometer (for **4** at the CLRC Daresbury synchrotron, SRS station 9.8, $\lambda = 0.6881$ Å). Data collection and structure refinement was achieved using standard Bruker AXS control and integration software and SHELXTL for all compounds.

For **1** the structure was solved by direct methods. The asymmetric unit contains two molecules and two thf solvent molecules. C36 and C37 were disordered over two sites each, whose occupancies were constrained to sum to 1.0, with isotropic thermal parameters constrained to be equal, and restraints on the bond lengths. The non-H atoms were refined anisotropically, except for the disordered atoms. H-atoms were included in calculated positions, except for H1 and H40, which were found by difference Fourier techniques and refined isotropically.

For **2** the structure was solved by direct methods with one molecule in the asymmetric unit. The non-H were refined anisotropically and all H atoms were found by difference Fourier techniques and refined isotropically.

The structure of complex **4** was solved by direct methods. The asymmetric unit contains half a molecule of **4** and half

a molecule of dichloromethane. The non-H atoms were refined anisotropically and H atoms were included in calculated positions.

For **5** the structure was solved by the Patterson method. The asymmetric unit contains the molecule, together with 0.5 MePh disordered over two sites related by a centre of symmetry. The non-H atoms were refined anisotropically. H atoms, except those on the solvent molecule, were included in calculated positions. H1 was found by difference Fourier techniques and refined isotropically.

CCDC reference numbers 209174–209177.

See <http://www.rsc.org/suppdata/dt/b3/b304602h/> for crystallographic data in CIF or other electronic format.

Computational details section

All structural optimisations and electronic calculations were performed using the Gaussian98³⁴ suite of programs using a DFT approach the hybrid Becke³⁵ exchange functional and correlation function of Lee, Yang and Parr³⁶ were used, standard Gaussian98 convergence criteria were applied. On the uranium centre the energy-consistent small-core RECP (Relativistic Effective Core Pseudo-potential) with the corresponding optimized basis set of the Stuttgart group was used,³⁷ and for all remaining light elements a 6-31G* basis set was employed. The gOpenMol package^{38,39} was used to plot the HOMO electron densities at a contour value of 0.08.

References

- 1 R. G. Denning, *Struct. Bonding (Berlin)*, 1992, **79**, 215.
- 2 R. G. Denning, J. C. Green, T. E. Hutchings, C. Dallera, A. Tagliaferri, K. Giarda, N. B. Brookes and L. Braicovich, *J. Chem. Phys.*, 2002, **117**, 8008.
- 3 S. Matsika, Z. Zhang, S. R. Brozell, J.-P. Blaudeau, Q. Wang and R. M. Pitzer, *J. Chem. Phys. A*, 2001, **105**, 3825.
- 4 N. Kaltsoyannis, *Chem. Soc. Rev.*, 2003, **32**, 9.
- 5 D. L. Clark, S. D. Conradson, R. J. Donohoe, D. W. Keogh, D. E. Morris, P. D. Palmer, R. D. Rogers and C. D. Tait, *Inorg. Chem.*, 1999, **38**, 1456.
- 6 S. P. McGlynn, J. K. Smith and W. C. Neely, *J. Chem. Phys.*, 1961, **35**, 105.
- 7 C. Nguyen-Trung, G. M. Begun and D. A. Palmer, *Inorg. Chem.*, 1992, **31**, 5280.
- 8 R. A. Andersen, *Inorg. Chem.*, 1979, **18**, 209.
- 9 C. J. Burns, D. C. Smith, A. P. Sattelberger and H. B. Gray, *Inorg. Chem.*, 1992, **31**, 3724.
- 10 D. M. Barnhart, C. J. Burns, N. N. Sauer and J. G. Watkin, *Inorg. Chem.*, 1995, **34**, 4079.
- 11 C. J. Burns and A. P. Sattelberger, *Inorg. Chem.*, 1988, **27**, 3692.
- 12 C. J. Burns and A. P. Sattelberger, *Inorg. Chem.*, 2000, **39**, 5277.
- 13 M. J. Sarsfield, M. Helliwell and D. Collison, *Chem. Commun.*, 2002, 2264.
- 14 S. Al-Benna, M. J. Sarsfield, M. Thornton-Pett, D. L. Ormsby, P. J. Maddox, P. Bres and M. Bochmann, *J. Chem. Soc., Dalton Trans.*, 2000, 4247.
- 15 K. Aparna, R. McDonald, M. Ferguson and R. G. Cavell, *Organometallics*, 1999, **18**, 4241.
- 16 R. P. K. Babu, K. Aparna, R. McDonald and R. G. Cavell, *Organometallics*, 2001, **20**, 1451.
- 17 M. T. Gamer, S. Dehnen and P. W. Roesky, *Organometallics*, 2001, **20**, 4230.
- 18 A. Kasani, R. McDonald and R. G. Cavell, *Organometallics*, 1999, **18**, 3775.
- 19 P. R. Wei and D. W. Stephan, *Organometallics*, 2002, **21**, 1308.
- 20 M. P. Wilkerson, C. J. Burns, R. T. Paine and B. L. Scott, *Inorg. Chem.*, 1999, **38**, 4156.
- 21 R. Hasselbring, H. W. Roesky, A. Heine, D. Stalke and G. M. Sheldrick, *Z. Naturforsch., B: Chem. Sci.*, 1992, **48b**, 43.
- 22 H. Noeth and L. Meinel, *Z. Anorg. Allg. Chem.*, 1967, **349**, 225.
- 23 S. Sitran, D. Fregona, U. Casellato, P. A. Vigato, R. Graziani and G. Faraglia, *Inorg. Chim. Acta*, 1987, **132**, 279.
- 24 C. J. Burns, D. L. Clark, R. J. Donohoe, P. B. Duval, B. L. Scott and C. D. Tait, *Inorg. Chem.*, 2000, **39**, 5464.
- 25 R. E. Cramer, R. B. Maynard, J. C. Paw and J. W. Gilje, *J. Am. Chem. Soc.*, 1981, **103**, 3589.

- 26 R. E. Cramer, R. B. Maynard and J. W. Gilje, *Inorg. Chem.*, 1981, **20**, 2466.
- 27 T. J. Marks, *J. Organomet. Chem.*, 1978, **158**, 3325.
- 28 P. G. Allen, J. J. Bucher, D. L. Clark, N. M. Edelstein, S. A. Ekberg, J. W. Gohdes, E. A. Hudson, N. Kaltsoyannis, W. W. Lukens, M. P. Neu, P. D. Palmer, T. Reich, D. K. Shuh, C. D. Tait and B. D. Zwick, *Inorg. Chem.*, 1995, **34**, 4797.
- 29 L. H. Jones, *Spectrochim. Acta*, 1959, **11**, 409.
- 30 L. H. Jones, *Spectrochim. Acta*, 1958, **10**, 395.
- 31 R. G. Denning, O. J. Norris, I. G. Short, T. R. Snellgrove and D. R. Woodward, *Lanthanide and Actinide Chemistry and Spectroscopy*, ed. N. M. Edelstein, American Chemical Society, Washington DC, 1980.
- 32 R. G. Denning, T. R. Snellgrove and D. R. Woodward, *Mol. Phys.*, 1976, **32**, 419.
- 33 R. Appel and I. Ruppert, *Z. Anorg. Allg. Chem.*, 1974, **406**, 131.
- 34 M. J. Frisch, G. W. Trucks, H. B. Schlegel, G. E. Scuseria, M. A. Robb, J. R. Cheeseman, V. G. Zakrzewski, J. A. Montgomery, R. E. Stratmann, J. C. Burnant, S. Dapprich, J. M. Millam, A. D. Daniels, K. N. Kudin, M. C. Strain, O. Farakas, J. Tomasi, V. Barone, M. Cossi, R. Cammi, B. Mennucci, C. Pomelli, C. Adamo, S. Clifford, J. Ochterski, G. A. Petersson, P. Y. Ayala, Q. Cui, K. Morokuma, D. K. Malick, A. D. Rabuck, K. Raghavachari, J. B. Foresman, J. Cioslowski, J. V. Ortiz, B. B. Stefanov, G. Lui, A. Liashenko, P. Piskorz, I. Komaromia, R. Gomperts, R. L. Martin, D. J. Fox, T. Keith, M. A. Al-Laham, C. Y. Peng, A. Nanayakkara, C. Gonzalez, M. Challacombe, P. M. W. Gill, B. G. Johnson, W. Chen, M. W. Wong, J. L. Andres, M. Head-Gordon, E. S. Replogle, J. A. Pople, in 'Gaussian 98', Pittsburgh PA., 1998.
- 35 A. D. Becke, *Phys. Rev. A*, 1988, **38**, 3098.
- 36 J. P. Perdew, K. Burke and Y. Wang, *Phys. Rev. B*, 1996, **54**, 16533.
- 37 W. Kuchle, M. Dolg, H. Stoll and H. Preuss, *J. Chem. Phys.*, 1994, **100**, 7535.
- 38 L. Laaksonen, *J. Mol. Graph.*, 1992, **10**, 33.
- 39 D. L. Bergman, L. Laaksonen and A. Laaksonen, *J. Mol. Graph. Model.*, 1997, **15**, 301.